# Pressure Variation Model of an Underwater Vehicle through Multiple Motions using CFD simulation

Thi Loan MAI*, Thi Thanh Diep NGUYEN*, Aeri CHO*, Sojin KWON*, Namug HEO*, Sanghyun KIM*, Ji-Hye KIM**, and Hyeon Kyu YOON**
*Changwon National University, Changwon-si, Gyeongsangnam-do, 51140 Korea
hkyoon@changwon.ac.kr

Key words: pressure variation model, dynamic pressure, computational fluid dynamic, submerged body

**ABSTRACT**

An underwater vehicle operates efficiently in the water environment when it determines the speed and direction. In this article, we investigate the pressure variation model (PVM) of an underwater vehicle to predict its speed and direction. A series of pressure sensors located at the port and starboard sides along the submerged body is used to measure the variation of pressure surrounding the body. The dynamic pressure is a selection to consider as a function of the flow velocity acting on each pressure sensor. Due to the good accuracy and flexibility in motion simulation of the CFD (computational fluid dynamics) method, it is applied to execute the submerged vehicle motions from simple to complexes such as rectilinear, turning, gliding, and spiral motions. For each motion, motion variables including linear velocity, angular velocity, and angle are given to describe the trajectory as well as the characteristics of motions. Based on the results of pressure variation, pressure are big changed for the position the head and rear of AUV. The PVM is established considering the motion variables and positions of the pressure sensors. The PVM proposed is also used to determine the motion variables.

## 1. Introduction

Nowadays, with needs in activities of scientific research, military, and commercial fields, submerged bodies vehicles have become essential systems widely. Navy has developed numerous submerged bodies, and AUV is paid attention to due to its application in many fields such as hydrographic survey, geographic mapping, sampling, construction, maintenance of structures, and so on. Therefore, it is necessary to predict correctly its navigation as well as its position during the mission process.

In the past, the localization of underwater vehicles was investigated based on pressure sensors. Chambers et al. (2014) used the instrument with pressure sensors on a three-dimensional fish-shaped head to investigate the pressure signal for relevant hydrodynamic stimuli to an ALLS. The pressure sensors provided information about the environment such as the source of flow fluctuation, the size of the source, and so non. Liu et al. (2016) introduced artificial lateral line sensors to measure the pressure and its application in hydrodynamic detection such as flow regime discrimination, velocity estimation, flow direction detection, object identification, and robot control strategy. Wang et al. (2016) used an artificial lateral line to precisely evaluate the speed of a freely swimming robot for the first time by massively experiments. Besides, Authors proposed a nonlinear prediction model to evaluate the speed of the robotic fish by analyzing distributed pressure, motion kinematics data, and speed of the robot. Liu et al. (2018) proposed the fish lateral line system should be applied to underwater environment perception and navigation, breaking the traditional detected way based on acoustic, optical, and inertial navigation. Zheng et al. (2020) experimented a freely swimming robotic fish in multiple motions to investigate the state. A pressure variation (PV) model for each motion that links motion parameters to PVs surrounding the robotic fish was established. As a result, the motion variables could be calculated using the PV model which was measured by artificial lateral line system (ALLSs). Additionally, a trajectory estimation method was proposed to determine the trajectory of robot fish based on the obtained motion variables.

This article focuses on the formulation of PVM of the AUV based on pressure measured by pressure sensors located at the starboard and port sides along AUV. The PVM is established for 6-DoF motion that link the motion variable consisting of linear velocity, angular velocity, and position. The motion variables are defined in straight, turning, gliding, and spiral motions which are easily performed using CFD simulation method. The pressures of pressure sensors obtained from straight, turning, gliding, and spiral motion are used to construct the regression model for each pressure sensor in each motion. Then, the coefficients in PVM are determined, and it can be used to complete the PVM which can estimate the velocity, direction, and localization of AUV.

## 2. Test overview

### 2.1 Objective

An autonomous underwater vehicle (AUV) used in this study is a slender body with a shape of of REMUS. The

main dimension is 1.34 m in length, 0.191 m in diameter. Fig. 1(a) shows the AUV's shape. A series of pressure sensors (red color) with a diameter of 0.01 m is located at the starboard and port sides along the AUV. Each pressure sensor is named and positioned as described in Fig. 1(b) where R and L indicate the pressure sensors on the starboard (right) and port (left) sides, respectively. To obtain the PVM, different kinds of tests of straight, turning, and gliding tests are performed to measure the pressure sensors. Table 1 depicts the test condition in this study.

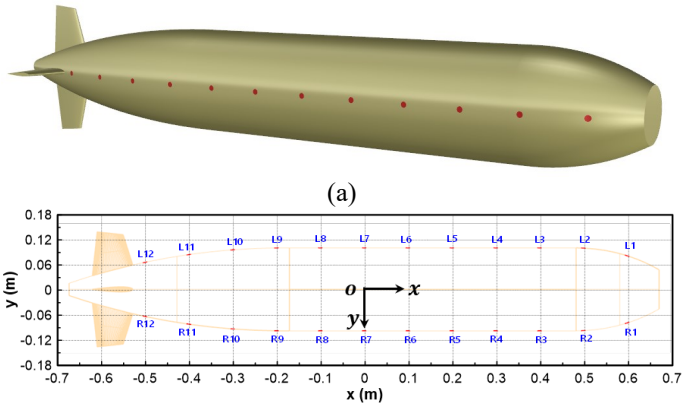

Fig. 1 AUV shape and pressure sensor position.

Table 1 Test condition

| Motion | Motion variable | Note |
|---|---|---|
| Straight | U = 0.5, 1.0, 1.5, 2.0, 2.5, 3.0, 3.5, 4.0 (knots) | $\omega = 0$<br>$\theta = 0$ |
| Turning | U = 2.0, 3.0, 4.0 (knots)<br>r = 10, 20, 30 (deg./s) | $\omega \neq 0$<br>$\theta = 0$ |
| Gliding | U = 2.0, 3.0, 4.0 (knots)<br>$\theta$ = 5, 10, 15, 20, 25, 30 (deg.) | $\omega = 0$<br>$\theta \neq 0$ |

### 2.2 CFD simulation

The governing equation consists of the mass and momentum conservation equation. The URANS (Unsteady Reynolds Averaged Navier-Stokes) approach is used to solve the governing equation. The assumption, the flow is incompressible, the governing equation is expressed as follows:

$$\frac{\partial \overline{u}_i}{\partial x_i} = 0 \tag{1}$$

$$\frac{\partial \overline{u}_i}{\partial t} + \overline{u}_j \frac{\partial \overline{u}_i}{\partial \overline{u}_j} = f_i - \frac{1}{\rho}\frac{\partial \overline{p}}{\partial x_i} + \frac{1}{\rho}\frac{\partial}{\partial x_j}\left(\mu \frac{\partial \overline{u}_j}{\partial x_j} - \rho \overline{u_i' u_j'}\right) \tag{2}$$

Here, $u_{i,j}$ $(i, j = 1, 2, 3)$ are the averaged velocity vector, $x_{i,j}$ $(i, j = 1, 2, 3)$ are the Cartesian coordinates, $\rho \overline{u_i' u_j'}$ is the Reynold stress, $\overline{p}$ is the averaged pressure, and $\mu$ is the viscosity coefficient of fluid.

The computational domain is designed following the ITTC recommended procedure (201), to be sufficiently large to avoid backflow and reflection. The physical condition is applied to the boundary domain, a velocity inlet is defined at the upstream, top, bottom, and sidewalls of the fluid domain. At the downstream, a pressure outlet is imposed. A no-slip wall is applied to the AUV. In addition, an ellipse cover surrounds the AUV as an overset region to execute the movement of the AUV in straight, turning, and gliding motion. The mesh generation was created automatically by meshing generator using the cut-cell method for volume and surface. A trimmed cell

mesher was applied to create the volume grids while the surface remesher was used to achieve a high-quality surface mesh. The boundary layer covers the AUV with ten layers of prismatic cells. During the simulation, the non-dimensional wall distance y+ value was maintained to lower than 1. The grid refinement was generated surrounding the AUV and region where AUV trajectory with travel using volumetric control to improve the calculation accuracy. Fig. 2 shows the overview of computational mesh, boundary condition, and boundary domain of straight, turning, and gliding motions. The AUV is simulated at a water depth of 7 m calculated from the free surface for straight and turning motion, and an initial water depth of 7 m for gliding motion.

The $k-\omega$ SST is widely used to simulate the flow of the marine vehicle due to its advantage in terms of CPU time and accuracy. The implicit unsteady method was applied throughout the simulation. The volume of fluid is the technique to define the Eulerian multiphase which separates two flow phases of water and air. A SIMPLE (Semi-Implicit Method for Pressure-Linked Equations) algorithm was applied to solve the governing equation iteratively, adjusting the pressure to ensure that the resulting velocity field satisfied continuity. The translation, rotation, and trajectory motion were defined for straight, turning, and gliding motion, respectively.

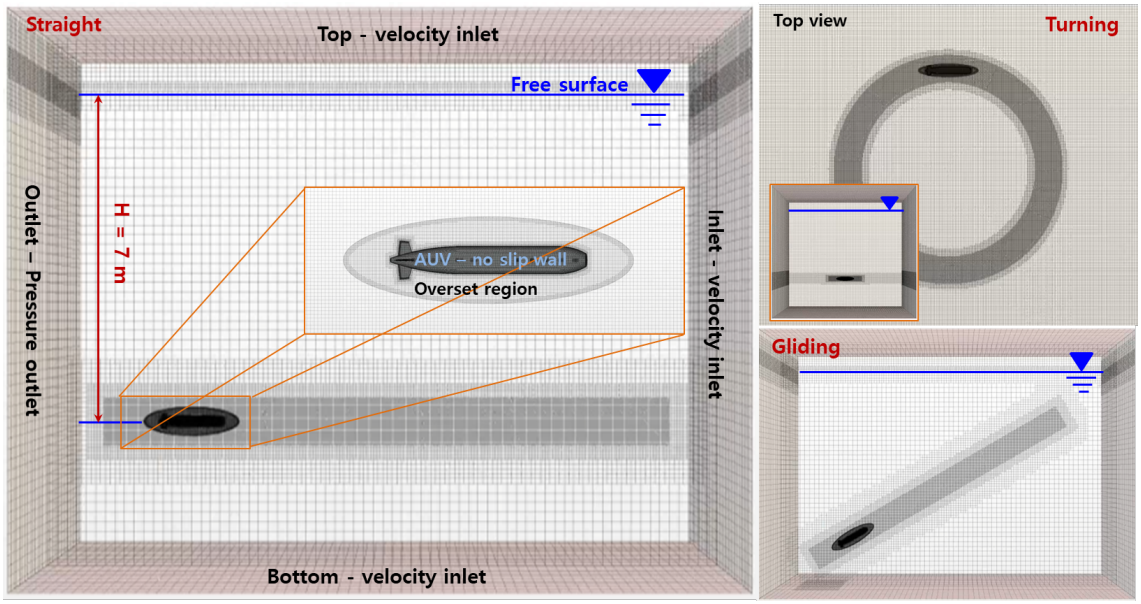


Fig. 2 Overview of computational mesh and boundaries.

## 3. Pressure variation model (PVM)

The motion of the body-fixed coordinate system ($o-xyz$) is described relative to an inertial reference frame while an earth-fixed coordinate system ($O-XYZ$) can be considered to be inertial. Therefore, the position and orientation of the marine vehicle are described relative to the inertial reference frame, while linear and angular velocities are expressed in the body-fixed coordinate system. The motion variables of the marine vehicle considered as know values are defined according to SNAME (1950) notation as velocity at origin $\underline{v}_0 = \begin{bmatrix} u & v & w \end{bmatrix}^T$, angular velocity $\underline{\omega} = \begin{bmatrix} p & q & r \end{bmatrix}^T$, and the body in the specific position $\underline{r}_p = \begin{bmatrix} x_p, y_p, z_p \end{bmatrix}^T$. The estimated speed ($V$) of the body at a specific position which is derived from velocity ($\underline{v}_p$) is expressed in Eq. (4).

$$\underline{v}_p = \underline{v}_0 + \underline{\omega} \times \underline{r}_p = \begin{bmatrix} u \\ v \\ w \end{bmatrix} + \begin{vmatrix} i & j & k \\ p & q & r \\ x & y & z \end{vmatrix} = \begin{bmatrix} u + zq - yr \\ v + xr - zp \\ w + yp - xq \end{bmatrix} \tag{3}$$

$$
\begin{aligned}
V^2 &= \left(u + zq - yr\right)^2 + \left(v + xr - zp\right)^2 + \left(w + yp - xq\right)^2 \\
&= u^2 + z^2q^2 + y^2r^2 + 2zuq - 2yur - 2zyqr \\
&+ v^2 + x^2r^2 + z^2p^2 + 2xvr - 2zvp - 2xzrp \\
&+ w^2 + y^2p^2 + x^2q^2 + 2ywp - 2xwq - 2yxpq
\end{aligned} \tag{4}
$$

Here, *u,v,* and *w* are surge, sway, and heave velocity, respectively; *p,q*, and *r* denote the roll, pitch, and yaw angular velocity, respectively; *x, y*, and *z* indicate the position with the earth-fixed coordinate system; *i, j,* and *k* refer the unit vector with the body-fixed coordinate system.

Depth of the body at a specific position is derived from Euler transformation which is mentioned by Fossen (1994) for 321 Euler transformation as Eq. (5). Expressing the body at a specific position with respect to the earth-fixed coordinate system in Eq. (6), the depth (*Z*) of the body at a specific position for the marine vehicle is written in Eq. (7)

$$
C_b^m = \begin{bmatrix} c\psi c\theta & -s\psi c\phi + c\psi s\theta s\phi & s\psi s\phi + c\psi c\phi s\theta \\ s\psi c\theta & c\psi c\phi + s\phi s\theta s\psi & -c\psi s\phi + s\theta s\psi c\phi \\ -s\theta & c\theta s\phi & c\theta c\phi \end{bmatrix} \tag{5}
$$

$$
\underline{R} = \underline{R}_0 + C_b^n \underline{r} \tag{6}
$$

$$
Z = Z_0 - x\sin\theta + y\cos\theta\sin\phi + z\cos\theta\cos\phi \tag{7}
$$

Where, $C_b^m$ is the transformation matrix from body-fixed coordinate system to earth-fixed coordinate system; s and c denote the sine and cosine; $\phi$, $\theta$, and $\psi$ indicate the attitude of the vehicle.

The hydrodynamic PVs (pressure variation) of the pressure sensor on the surface of the AUV can be considered as the gauge pressure in Eq. (8).

$$
P_g = P_d + P_s = \frac{\rho}{2}V_f^2 + \rho g Z \tag{8}
$$

The perturbation theory organize up to $O\left(\varepsilon^2\right)$ is applied to calculate pressure of the pressure sensor. In generally, considering 6-DoF (Degree of Freedom) states with $O(1) = \begin{bmatrix} u & x \end{bmatrix}$ and $O(\varepsilon) = \begin{bmatrix} v & w & p & q & r & y & z & \phi & \theta \end{bmatrix}$, the speed and depth of pressure sensor are calculated as Eqs. (9) and (10) respectively.

$$
V^2 = u^2 + 2zuq - 2yur + v^2 + x^2r^2 + 2xvr + w^2 + x^2q^2 - 2xwq \tag{9}
$$

$$
Z = Z_0 - x\theta + y\phi + z \tag{10}
$$

For straight motion, the motion variables and position are defined as $u \neq 0$, $v = 0$, $w = 0$, $q = 0$, $r = 0$, $x = 0$, $y = 0$, and $z \neq 0$. Therefore, the speed and depth of pressure sensor in straight motion are calculated in Eqs. (11) and (12).

$$
V^2 = u^2 \tag{11}
$$

$$
Z = Z_0 + z \tag{12}
$$

Similarly for turning motion, with $u \neq 0$, $v = 0$, $w = 0$, $q = 0$, $r \neq 0$, $x = 0$, $y = 0$, and $z \neq 0$, the speed and depth of pressure sensor in turning motion are expressed in Eqs. (13) and (14).

$$
V^2 = u^2 - 2yur + x^2r^2 \tag{13}
$$

$$Z = Z_0 + z \tag{14}$$

By the same way, in gliding motion, motion variables of AUV are similar to straight motion with $u \neq 0$, $v = 0$, $w = 0$, $q = 0$, and $r = 0$ while the position is defined with $x \neq 0$, $y = 0$, and $z \neq 0$. Hence, the speed and depth of the pressure sensor are calculated during gliding motion as in Eq. (15) and (16).

$$V^2 = u^2 \tag{15}$$

$$Z = Z_0 - x\theta + z \tag{16}$$

To establish the regression model for PVM , the motion variables in Eqs. (9) and (10) are known that $x$, $y$, and $z$ are the design position of the pressure sensors. $u^2 + v^2 + w^2 + Z_0$ can not be estimated separately, so it is collectively referred to $VZ_0$. Thus, motion variables for PVM are reduced with motion variables of $VZ_0$, $uq$, $ur$, $r^2$, $vr$, $q^2$, $wq$, $\theta$, and $\phi$. On the other hand, to determine the speed and direction of the AUV, a pressure difference ($P_{residual}$) is used. Pressure difference describes the value among the hydrostatic pressure component removed from the measured pressure as written in Eq. (17).

$$P_{residual} = P - \rho g z \tag{17}$$

The flow velocity ($V_f$) at a specific position is a function of body motion and the design position of the pressure sensors. It is assumed that the geometric shape can be determined by the regression coefficients of each term. The PVM is expressed in Eq. (18) for pressure sensors.

$$P_{residual} = \begin{bmatrix} VZ_0 & 2z_1uq & -2y_1ur & x_1^2r^2 & 2x_1vr & x_1^2q^2 & -2x_1wq & -x_1\theta & y_1\phi \\ VZ_0 & 2z_2uq & -2y_2ur & x_2^2r^2 & 2x_2vr & x_2^2q^2 & -2x_2wq & -x_2\theta & y_2\phi \\ \cdots & \cdots & \cdots & \cdots & \cdots & \cdots & \cdots & \cdots & \cdots \\ VZ_0 & 2z_9uq & -2y_9ur & x_9^2r^2 & 2x_9vr & x_9^2q^2 & -2x_9wq & -x_9\theta & y_9\phi \end{bmatrix} \begin{bmatrix} \alpha_{VZ} \\ \alpha_{uq} \\ \alpha_{ur} \\ \alpha_{rr} \\ \alpha_{vr} \\ \alpha_{qq} \\ \alpha_{wq} \\ \beta_{\theta} \\ \beta_{\phi} \end{bmatrix} \tag{18}$$

Where, $-2ur + \phi$, $r^2 + q^2$, $2vr - 2wq$, and $2vr - 2wq - \theta$ can not be defined. Therefore, it is necessary to a regression through several motion calculations of straight, turning, gliding, and spiral.

## 4. Results and discussion

Fig. 3 shows the pressure sensors at various speeds in straight motion. Pressure does not change so much at the pressure sensors located at the position where the curvature of AUV is not changed as sensors from R3 to R8. Other pressure sensors are located at the position where the curvature of AUV varies, the pressures give a big change, especially the pressure sensor at the head of AUV are R1, R2, and at the rear of AUV is R12 even R12 is opposite direction compared with other sensors. Due to different speeds, the pressure of each pressure sensor describes a second-order function of speed as Eq. (19). Therefore, it is easy to obtain the coefficient of $\alpha_{VZ}$ and $C$ for pressure, where $\alpha_{VZ}$ is $u^2$ in straight motion. Plotting coefficients $\alpha_{VZ}$ and $C$ for each pressure sensor versus their position on AUV in Fig. 4, the coefficient of $\alpha_{VZ}$ changes based on the pressure magnitude of sensors, and coefficients of C are a constant with every pressure sensors.

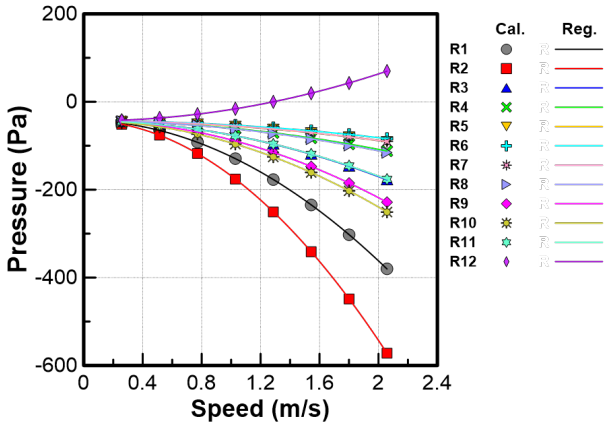

Fig. 3 Pressure of each pressure sensor at various speeds of straight motion.

$$P = VZ_0\alpha_{vz} + C \tag{19}$$

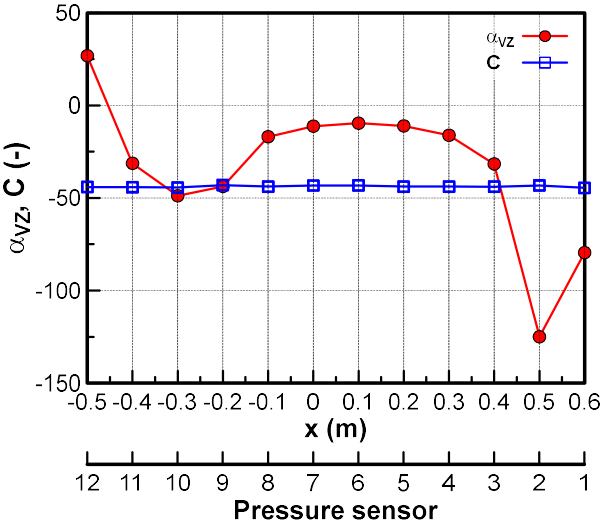

Fig. 4 Coefficient of pressure sensors versus their position along AUV in straight motion.

Fig. 5 presents the pressure sensors at various speeds and turning rates in turning motion. Due to asymmetry flow acting on the starboard and port sides of AUV, pressure sensors on the port side are also depicted to compare the difference with pressure sensors on the starboard side. Pressure on the starboard side is observed to be greater than the port side for the pressure sensor located at mid-body where the curvature of AUV is not changed or small changed as sensors 3-10 due to flow velocity strongly acting on the starboard side. The results at a turning rate of 0 are results of straight motion. Eq. (20) describes the regression model of pressure sensors in turning motion, where $VZ_0$ is $u^2$ which similar results with straight motion, so the term $VZ_0\alpha_{VZ}$ is subtracted to obtain the coefficients relative to turning rate ($r$). Fig. 6 shows the coefficients of pressure sensors versus their position along AUV in turning motion. When the position of the pressure sensors is not mentioned in Fig. 6(a), the coefficient $\alpha_{ur}$ of pressure sensors in the starboard and port sides is observed to be nearly symmetry via a value of 0, while coefficient $\alpha_{rr}$ in both sides is positive except to sensor L3 is negative. When the position of the pressure sensors is considered in Fig. 6(b) , the coefficient $\alpha_{ur}$ is similar between sensors on the starboard and port sides, and $\alpha_{ur}$ value is not varied at the pressure sensor located at the mid-body (sensors 3-9). The coefficient $\alpha_{rr}$ has a big change, especially sensors 5, 6, and 7. $\alpha_{rr}$ becomes zero at sensor 7 because sensor 7 is located at the mid-body, so the $x$-position of sensor 7 is zero. The coefficient C is a constant value at every pressure sensors.

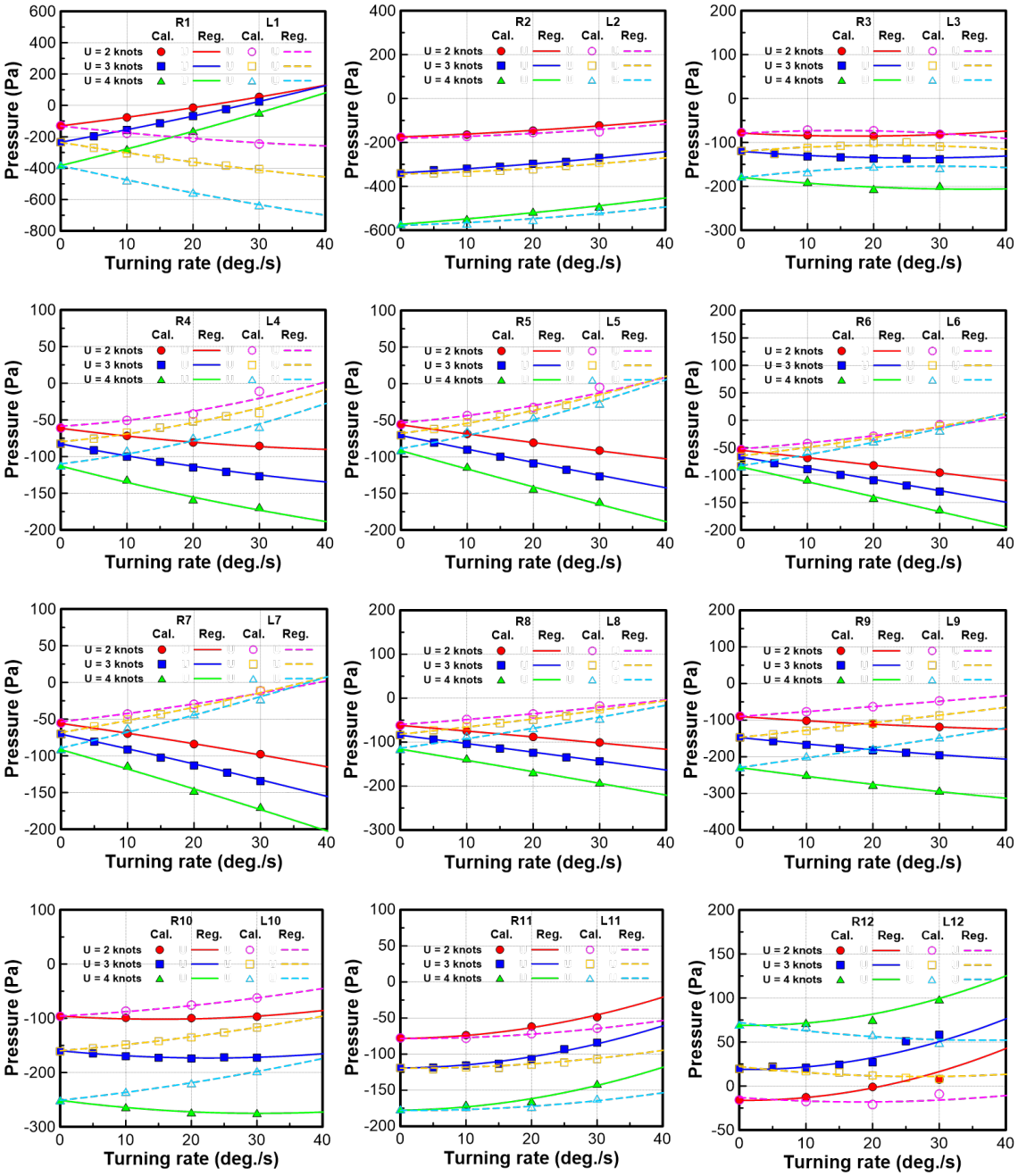


Fig. 5 Pressure of each sensor at various speeds and turning rates of turning motion.

$$P = VZ_0\alpha_{vz} - 2yur\alpha_{ur} + x^2r^2\alpha_{rr} + C \tag{20}$$

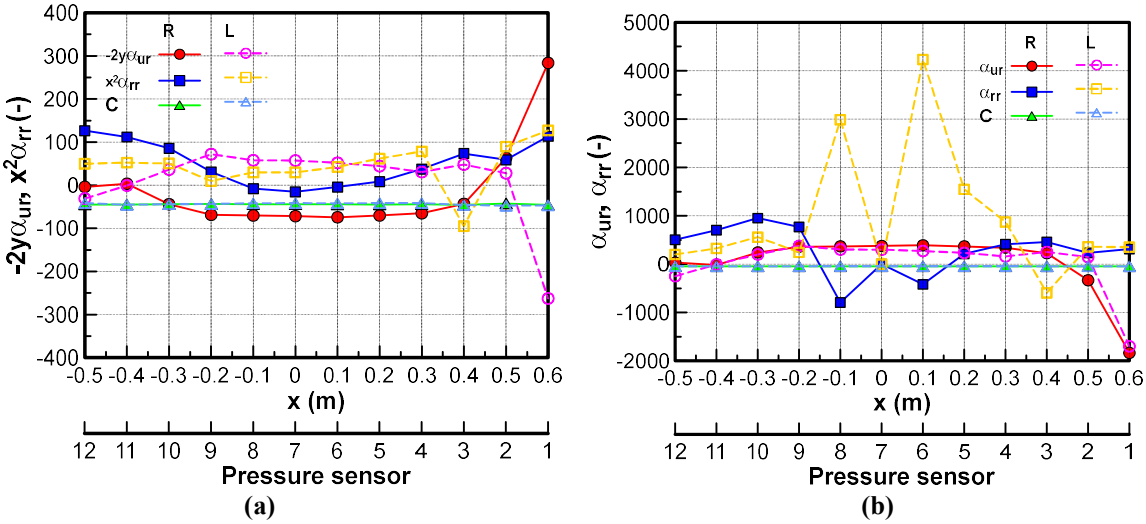


Fig. 6 Coefficient of pressure sensors versus their position along AUV in turning motion: (a) When the position of sensors is not mentioned; (b) When the position of sensors is mentioned.

Fig. 7 shows the pressure of pressure sensors in gliding motion which is performed at various pitch angles and a constant speed of 3 knots. It can be seen that pressure is nearly similar for each pressure sensor due to different pitch angles and it is the same with straight motion at speed of 3 knots which a pitch angle is 0. Therefore, there is no discrimination due to pitch angle, and the influent of pitch angle in gliding motion can be ignored. The relationship between pitch angle and pressure sensors will be found in the spiral motion in future work.

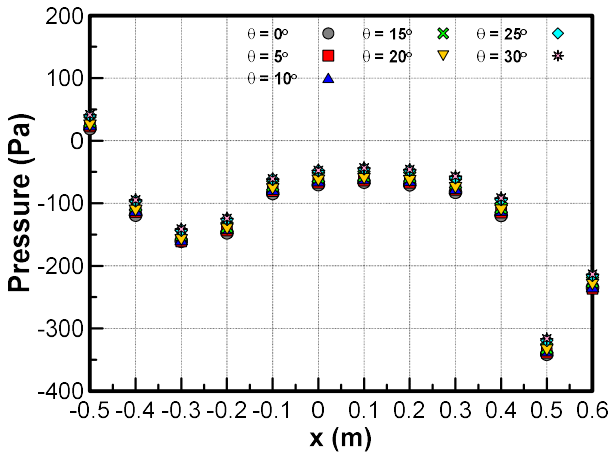


Fig. 7 Pressure of each sensor at various pitch angles.

Table 2 lists the coefficients of the pressure sensors in the straight and turning motion. It can be used to alternate into Eq. (18) for completing the PVM which can determine the speed, direction, and depth of AUV based on pressure.

Table 2 Coefficient of pressure sensors in straight and turning motion

| Pressure sensor | Straight motion | | Turning motion | | |
|---|---|---|---|---|---|
| | $\alpha_{vz}$ | $C_s$ | $\alpha_{ur}$ | $\alpha_{rr}$ | $C_t$ |
| R1 | -79.504 | -44.578 | -1835.512 | 314.722 | -45.749 |
| R2 | -124.994 | -43.259 | -333.045 | 235.428 | -42.249 |
| R3 | -31.610 | -43.935 | 226.911 | 459.500 | -45.288 |
| R4 | -16.151 | -43.855 | 341.958 | 414.333 | -44.278 |
| R5 | -11.091 | -43.857 | 367.857 | 210.405 | -44.518 |
| R6 | -9.617 | -43.234 | 389.598 | -419.210 | -44.375 |
| R7 | -11.232 | -43.266 | 376.303 | 0.000 | -43.890 |
| R8 | -16.932 | -43.885 | 367.710 | -792.040 | -43.984 |

| | | | | | |
|---|---|---|---|---|---|
| R9 | -43.775 | -43.026 | 360.212 | 769.200 | -43.688 |
| R10 | -48.821 | -44.402 | 242.486 | 951.289 | -43.915 |
| R11 | -31.298 | -44.167 | -21.279 | 699.938 | -44.953 |
| R12 | 26.799 | -44.080 | 31.411 | 505.600 | -44.692 |
| L1 | -79.504 | -44.578 | -1699.948 | 353.167 | -46.625 |
| L2 | -124.994 | -43.259 | 147.065 | 358.524 | -47.472 |
| L3 | -31.610 | -43.935 | 251.856 | -593.388 | -45.766 |
| L4 | -16.151 | -43.855 | 160.035 | 871.611 | -41.374 |
| L5 | -11.091 | -43.857 | 232.647 | 1547.150 | -41.607 |
| L6 | -9.617 | -43.234 | 272.004 | 4232.400 | -41.837 |
| L7 | -11.232 | -43.266 | 299.927 | 0.000 | -41.552 |
| L8 | -16.932 | -43.885 | 303.177 | 2984.600 | -41.895 |
| L9 | -43.775 | -43.026 | 377.886 | 242.790 | -43.396 |
| L10 | -48.821 | -44.402 | 200.440 | 560.144 | -44.054 |
| L11 | -31.298 | -44.167 | -4.578 | 326.994 | -45.261 |
| L12 | 26.799 | -44.080 | -249.402 | 199.800 | -41.460 |

## 5. Conclusion

This study presented the formulation of PVM which can determine the speed and direction of the AUV based on pressure measured by pressure sensors. The formulation of PVM was established for 6-DoF motion that kink the motion variables including linear velocity, angular velocity, position, and the depth model was derived from 321 Euler transformation. Therefore, the motion variables of pressure sensors were defined in straight, turning, gliding, and spiral motion. By giving the motion variable for each motion, the regression model of flow velocity and depth of submerged body was determined for each motion. A series of pressure sensors were located at the starboard and port sides along the AUV to measure the pressure surrounding the body. The pressure was estimated using CFD simulation method in STAR CCM+ due to good accuracy and flexibility in motion simulation. The straight, turning, and gliding motion was performed by applying the translation, rotation, and trajectory motion, respectively. In straight motion, pressure was not varied so much at sensors located at the mid-body where the curvature of AUV is not changed. The pressure gave a big change observed for sensor located at the head and rear of AUV. A second-order function of speed was found for the pressure of each sensor due to different speeds in straight motion. For turning motion, the pressure on the starboard side was greater than the port side for the sensor located at the mid-body due to flow velocity strongly acting on the starboard side. For gliding motion, the pressure was observed to not vary so much due to different pitch angles. Therefore, the effect of pitch angle in gliding motion could be ignored, and the relationship between pitch angle and pressure sensors will be found in spiral motion in future work. By regression model of each pressure sensor in straight and turning motion, the coefficients in PVM were determined. It can be used to complete the PVM which can estimate the velocity, direction, and depth of AUV.

## Acknowledgment

This research was supported by a grant from Endowment Project of "Development of smart sensor technology for underwater environment monitoring" funded by Korea Research Institute of Ships and Ocean engineering (PES4400).

## References

(1)Fossen, T. (1994): Guidance and Control of Ocean Vehicles. Book.
(2) ITTC (2011). ITTC – Recommended Procedures and Guidelines: Practical Guidelines for Ship CFD Application, 7.5–03–02–03.
(3)Liu, G., Wang, A., Wang, X., and Liu, P. (2016): A review of Artificial Lateral Line in Sensor Fabrication and Bionic Applications for Robot Fish, Aookued Bionics and Biomechanics, Vol. (2016).
(4) Liu, G., Wang, M., Wang, A., Wang, S., Yang, T., Malekian, R., and Li, Z. (2018): Researcg on Flow Field Perception Based on Artificial Lateral Line Sensor System, Sensors 2018, Vol. (18).
(5)Wang, W., Li, Y., Zhang, X., Wang, C., Chen, S., and Xie, G. (2016) Speed Evaluation of a Freely Swimming Robotic Fish with an Artificial Lateral Line, 2016 IEEE International Conference on Robotics and Automation.

(6)Zheng,X., Wang,W., Xiong, M., and Xie, G. (2019): Online State Estimation of a Fin-Actuated Underwater Robot Using Artificial Lateral Line System, IEEE Transactions on Robotics.

**Author's Biography**

Thi Loan MAI and Thi Thanh Diep NGUYEN are Ph.D candidate students in the department of Smart Environmental Energy Engineering in Changwon National University, Korea. They got Engineer's degree in the department of Naval Architecture in Ho Chi Minh City University of Transport, Vietnam, in 2017 and master degree in department of Naval Architecture and Marine Engineering in Changwon National University, Korea, in 2019. Their main interests are seakeeping and maneuvering of marine vehicles.

Aeri CHO, Sojin KWOn, Namug HEO, and Sanghyun KIM are master candidate students in the department of Smart Environmental Energy Engineering in Changwon National University, Korea. They got bachelor in the department of Naval Architecture and Marine Engineering in Changwon National University, Korea.

Ji-Hye KIM is a professor in the department of Naval Architecture and Marine Engineering in Changwon National University, Korea.

Hyeon Kyu YOON is a professor in the department of Naval Architecture and Marine Engineering in Changwon National University, Korea. He got bachelor, master and Ph.D degrees in the department of Naval Architecture and Ocean Engineering in Seoul National University, Korea, in 1989, 1991, and 2003. He worked for Agency for Defence Development from 1991 to 1996, and worked for Maritime Ocean Engineering and Research Institute from 2003 to 2009. His main interests are the simulation of marine vehicles such as a ship and under vehicles, and the model test in the water tank.